Optimization of nozzle geometry for improving bottomhole cleaning efficiency in roller cone drilling

Dilobar Nazarbekova[1], **Bekzod Nurtoev**[2]
Tashkent State Technical University named after Islam Karimov, Tashkent, Uzbekistan
[1]Corresponding author
E-mail: [1]*amndk.nazarbekova@yandex.ru*, [2]*bekzodnurtoyev90@gmail.com*

Received 26 April 2026; accepted 4 June 2026; published online 16 July 2026
DOI https://doi.org/10.21595/vp.2026.26600

Check for updates

77th International Conference on Vibroengineering in Almaty, Kazakhstan, June 11-12, 2026

Abstract. This paper develops an engineering-analytical framework that links roller cone bit nozzle geometry directly to the specific hydraulic energy E_s required per metre drilled. A submerged free-jet decay relation, a cuttings-particle force balance and a Shields-type incipient-motion criterion are coupled to define the minimum wall-jet velocity for cuttings lift-off, which is imposed as a hard constraint in a constrained optimization of the nozzle diameter d_n, inclination angle θ and stand-off distance h. The problem is solved by parametric grid search and five representative configurations are compared. The recommended optimum ($d_n = 18$ mm, $\theta = 20°$, $h = 50$ mm) lowers E_s from 35.95 to 5.04 MJ/m (an 86 % reduction) and raises the predicted rate of penetration from 11.3 to 22.0 m/h (+95 %) relative to a conventional pressure-based arrangement, at the same flow rate and number of nozzles. A one-at-a-time sensitivity study confirms that the optimum is robust to the model calibration constants. Geometry-based redistribution of hydraulic energy is thus more effective, and more sustainable, than pressure-based intensification of the flushing flow.

Keywords: roller cone drilling, nozzle geometry, bottomhole cleaning, cuttings transport, specific hydraulic energy, nozzle optimization, energy-efficient drilling.

1. Introduction

Efficient bottomhole cleaning is a key factor in drilling performance, rate of penetration (ROP), bit durability and energy use. In roller cone drilling the flushing system must both deliver fluid to the bottomhole and rapidly remove cuttings from the destruction zone; if cuttings are not evacuated they are re-crushed, causing bit balling, hydraulic losses and tool wear. Nozzle shape and flushing organization strongly affect bottomhole performance [1], as do fluid properties and nozzle orientation [2]. Drilling efficiency depends not only on the energy supplied, but on how rationally it is distributed in rock destruction and cuttings transport [3]; a simple increase in pump pressure may merely raise dissipation and vortex circulation near the bottomhole.

Recent work emphasizes nozzle geometry and jet direction: extended/directional nozzles raise ROP by targeting the impact and improving evacuation [4], curved PDC-bit nozzles redistribute hydraulic energy and improve cleaning and cooling [10], and CFD–DEM studies confirm nozzle diameter, number and inclination as the most influential hydraulic parameters [11], [12]. Energy-efficient drilling is increasingly important because of power demand and carbon footprint [5], [6], [7], [13]. The incipient motion of cuttings is governed by drag, Saffman lift, gravity, buoyancy and inter-particle contact forces [14], [15]. The guiding principle here – improving performance by redistributing the available energy rather than increasing its total input – has methodological precedents in other domains, e.g. power-consumption modelling and optimization-based energy redistribution in traction-power systems [8], [9] (cited only as method analogies, not as drilling references).

The aim of this study is to develop and apply a quantitative rationale for optimizing nozzle geometry in roller cone drilling so as to improve cleaning while reducing specific hydraulic energy. Three specific contributions are made: (i) nozzle geometry is linked directly to the specific hydraulic energy $E_s = P_h/ROP$ rather than to absolute pressure or jet velocity, reformulating the design task as an energy-efficiency problem; (ii) a minimum wall-jet velocity u_{min} is derived from the particle force balance and used as a hard constraint; and (iii) a complete three-variable constrained optimization is solved numerically and verified against a conventional baseline.

2. Materials and methods

The framework couples an analytical hydrodynamic model with a numerical optimization of nozzle geometry in the bit-bottomhole zone. The flushing scheme and geometric factors are shown in Fig. 1: the nozzle diameter d_n, inclination angle θ (from the bit axis toward the wall), stand-off distance h, flow rate Q, nozzle pressure drop Δp, fluid density ρ, plastic viscosity μ and cuttings diameter d_p. In the optimized arrangement the orientation and flow path are chosen to direct the jet along the cuttings-removal path, not only at the rock face.

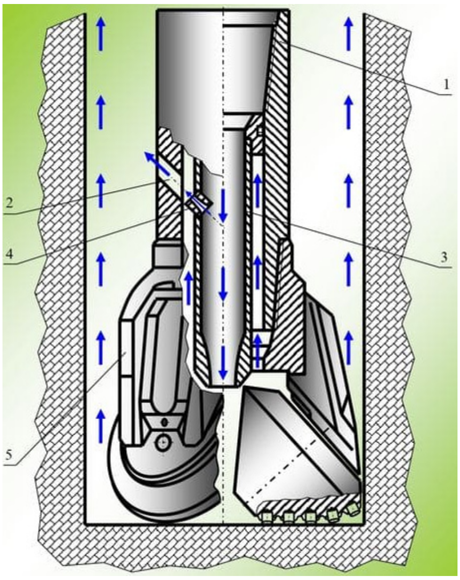

Fig. 1. General scheme of drilling fluid flow in the roller cone bit zone: 1 – drill string; 2 – side channel; 3 – central nozzle; 4 – nozzle; 5 – roller cone. Original figure prepared by the authors

For n nozzles of cross-section A_n, the outlet jet velocity follows from continuity and the nozzle pressure drop from a Bernoulli relation with discharge coefficient $C_d = 0.95$; the hydraulic power and total jet impact force are:

$$A_n = \frac{\pi d_n^2}{4}, \quad v_j = \frac{Q}{nA_n}, \tag{1}$$

$$\Delta p = \frac{\rho v_j^2}{2Cd^2}, \quad Ph = \Delta p \cdot Q, \quad F_j = \rho Q v_j. \tag{2}$$

Between the outlet and the bottomhole the jet behaves as a submerged turbulent free jet whose centreline velocity decays with distance; with a half-angle of spread $\alpha/2 = 6°$:

$$u(L) = \frac{v_j d_n}{\left[d_n + 2L\tan\left(\frac{\alpha}{2}\right)\right]}, \quad L = h. \tag{3}$$

For a nozzle tilted by θ, the radial (transport) component that sweeps cuttings toward the annulus is:

$$u_r = \max[u(L)\sin\theta, k_s u(L)], \quad k_s \approx 0.07, \tag{4}$$

so the radial component is non-zero even at $\theta = 0$ but is small. A single cuttings particle (d_p, ρ_p) lifts off when drag plus Saffman shear-lift [15] overcome the net submerged weight $F_p = \left(\frac{\pi}{6}\right) d_p^3(\rho_p - \rho)g$ and inter-particle friction (the force balance is shown in Fig. 2). A Shields-type criterion with combined friction–interlocking factor $K = 1.5$ gives the minimum radial velocity:

$$u_{min} = \sqrt{\left[\frac{2KF_p}{C_{d,p}\rho A_p}\right]}. \tag{5}$$

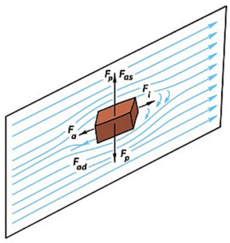

Fig. 2. Force interaction on a cuttings particle in the drilling-fluid flow: F_{ad} – drag; F_a – added-mass; F_{as} – Saffman shear-lift; F_i – inertial force; F_p – net submerged weight

With $\rho = 1200$, $\rho_p = 2600$ kg/m^3, $d_p = 3$ mm, $C_{d,p} = 0.44$, this gives $u_{min} \approx 0.40$ m/s. A higher transport (anti-balling) velocity $u_b \approx 8$ m/s is required to keep the bottomhole swept. The specific hydraulic energy and a two-stage cleaning map (lift-off margin $m_{lift} = u_r/u_{min}$, transport margin $m_{tr} = u_r/u_b$) are:

$$E_s = \frac{P_h}{ROP}, \quad \eta = 1 - \exp\left[-\frac{m_{lift} - 1}{k_c}\right], \tag{6}$$

$$ROP = ROP_{max}\eta(1 - \beta \cdot ball), \quad ball = \max[0, 1 - m_{tr}], \tag{7}$$

with $k_c = 1.5$, $\beta = 0.65$ and $ROP_{max} = 22$ m/h a representative formation ceiling. The calibration constants $(k_c, \beta, k_s, \alpha/2)$ are model parameters whose influence is tested in Section 3.4; $C_{d,p} \approx 0.44$ (sphere), $C_d = 0.95$ and the Saffman coefficient 1.615 [15] are standard literature values. The design problem is the constrained minimization:

$$\min E_s(X) = \Delta p(d_n, Q) \cdot \frac{Q}{ROP(X)}, \quad X = (d_n, \theta, h), \tag{8}$$

subject to g_1: $u_r \geq u_{\min}$ (cleaning); g_2: $\Delta p \leq \Delta p_{max} = 20$ MPa (pump); g_3: $F_j \geq 1000$ N (mechanical effect); and bounds $d_n \in [10, 18]$ mm, $\theta \in [0, 35]°$, $h \in [40, 80]$ mm. The non-convex problem was solved by parametric grid search (9×8 points at $h = 50$ mm), evaluating Eqs. (1-7) for each candidate and keeping the feasible point of lowest E_s; the fixed operational values are $Q = 30$ L/s and $n = 3$. The model was implemented in Python (NumPy/Matplotlib) and reproduces every entry of Table 1.

3. Results and discussion

3.1. Mechanism and force balance

Bottomhole cleaning cannot be judged by pressure drop or jet velocity alone. In a conventional scheme ($\theta = 0°$) the radial component arises only from wall-jet spreading (Eq. (4)), so cuttings linger and are re-crushed. With $\theta > 0$ the nozzle directly produces $u_r = u(L)\sin\theta$, one to two orders of magnitude larger, with no extra hydraulic power – the principal reason geometry outperforms pressure. For the reference particle the binding threshold is the transport velocity u_b= 8 m/s rather than $u_{\min} = 0.40$ m/s, so the geometry must raise u_r above u_b.

3.2. Comparison of representative configurations

Several conclusions follow (Table 1). Case A (large straight nozzle) uses only 30.8 kW but its radial velocity (1.42 m/s) is far below u_b, so balling occurs and ROP collapses to 8.4 m/h. Case B – the pressure-based response – triples Δp and P_h, yet u_r (5.27 m/s) still does not reach u_b; ROP recovers only to 11.3 m/h and E_s rises to 35.95 MJ/m, confirming that hydraulic intensification alone is the worst response to a cleaning problem. Cases C and D share $\theta = 20°$ and clear the constraint (ball = 0, ROP = 22 m/h), but D uses 3.7× less power because the larger 18 mm nozzle keeps Δp low while tilt supplies the radial momentum. Case E shows that further intensification beyond the optimum is purely wasteful.

Table 1. Quantitative comparison of conventional and optimized nozzle arrangements computed from Eqs. (1)–(7). Row D (highlighted) is the optimum from the parametric search

Case	Description	d_n, mm	θ, °	h, mm	v_j, m/s	Δp, MPa	P_h, kW	u_r, m/s	ROP, m/h	E_s, MJ/m
A	Conventional, large nozzle, straight ($\theta = 0°$)	18	0	80	39.3	1.03	30.8	1.42	8.4	13.15
B	Conventional, small nozzle, straight (pressure-based)	13	0	80	75.3	3.77	113.2	5.27	11.3	35.95
C	Tilt-only with small nozzle	13	20	50	75.3	3.77	113.2	14.25	22.0	18.52
D	Proposed optimum	18	20	50	39.3	1.03	30.8	8.49	22.0	5.04
E	Over-energized (small nozzle, strong tilt)	12	25	45	88.4	5.20	155.9	20.90	22.0	25.52

3.3. Optimization result

Fig. 3 shows E_s (solid) and ROP (dashed) versus inclination angle for four diameters at $h = 50$ mm. Three regions appear: a sub-feasible region ($\theta <$ ~10°) where balling dominates; an active region (~10-20°) where ROP rises steeply and E_s falls; and a saturation region ($\theta >$ ~20°) where ROP is at its ceiling. The global feasible optimum is $d_n = 18$ mm, $\theta = 20°$, $h = 50$ mm, with $E_s = 5.04$ MJ/m, ROP = 22 m/h, $\Delta p = 1.03$ MPa and $P_h = 30.8$ kW. Relative to the baseline (case A) the tilt alone cuts E_s by 62 % with no change in pressure or flow; relative to the pressure-based case B it cuts P_h by 73 % and E_s by 86 % while raising ROP by 95 %.

3.4. Sensitivity, boundary cases and limitations

Each input was varied by ±20 % at the optimum (Fig. 4). E_s and ROP are insensitive (≈ 0 %) to the particle density and to the calibration constants k_c, β, k_s and $\alpha/2$, because the optimum sits deep in the fully-cleaned regime; E_s scales linearly with mud density ρ and inversely with ROP_{max}, both physical inputs rather than fitted constants. Plastic viscosity μ does not enter the lift-off criterion and has no effect. The conclusions are therefore governed by geometry and measurable properties, not by the uncertain constants.

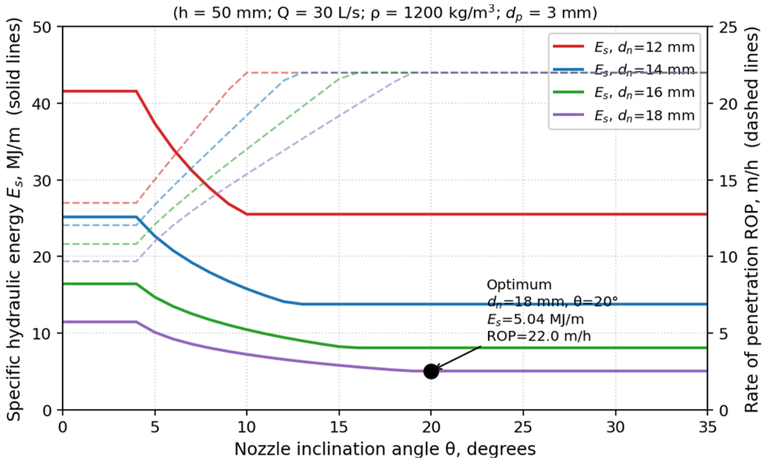

Fig. 3. Specific hydraulic energy E_s (solid) and predicted ROP (dashed) versus nozzle inclination angle θ for four nozzle diameters, at $h = 50$ mm, $Q = 30$ L/s, $\rho = 1200$ kg/m^3, $d_p = 3$ mm. The marker is the global feasible optimum

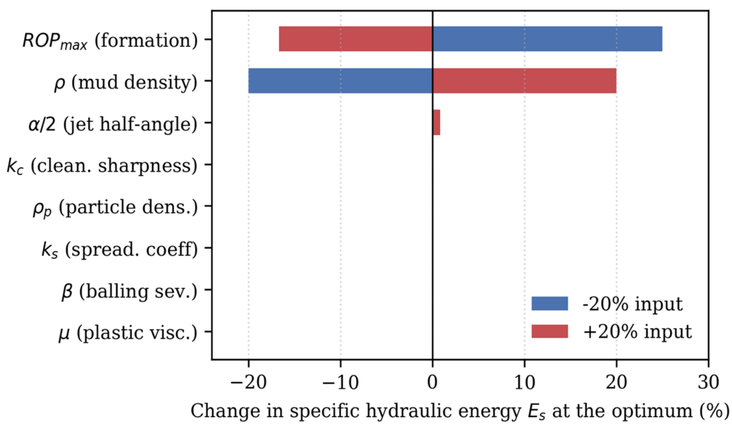

Fig. 4. Change in the specific hydraulic energy E_s at the optimum for a ±20 % change in each model input (tornado chart)

Two boundary cases were examined. In hard rock (low ROP_{max}) the geometry controls u_r independently of ROP_{max}, so the optimum d_n, θ do not shift; only the absolute E_s rises as $1/ROP_{max}$, and the saving over a straight jet persists. Under a pump-limited flow rate the minimum tilt to keep u_r above u_b rises (about 19° at 30 L/s to 29° at 20 L/s for an 18 mm nozzle); the energy-optimal response is to reduce the diameter (18 mm at 30 L/s to about 11 mm at 16 L/s), with E_s staying low (3-6 MJ/m). The design rule – increase tilt and trim diameter rather than raise pressure – therefore holds under pump constraints.

The results are from an analytical model not yet validated against experiment, CFD or field data; absolute ROP and E_s are design-screening estimates. The model assumes free-jet decay, a spherical-equivalent single-particle lift-off, steady flow and a formation-limited ROP ceiling, and neglects inter-particle jamming, multi-particle interaction, bit whirl, time-transient flow and non-Newtonian threshold effects. The sensitivity analysis mitigates this by showing robustness to the principal constants, but the validation programme below remains necessary before field use.

4. Conclusions

A closed model couples the nozzle outlet conditions, the submerged free-jet decay law, a

Saffman-corrected particle force balance giving the minimum lift-off velocity, and a two-stage cleaning map from wall-jet velocity to ROP. A three-variable constrained optimization (d_n, θ, h) with cleaning, pump and mechanical constraints was solved by grid search. The recommended optimum ($d_n = 18$ mm, $\theta = 20°$, $h = 50$ mm) reduces the specific hydraulic energy from 35.95 to 5.04 MJ/m (−86 %) and raises ROP from 11.3 to 22.0 m/h (+95 %) versus a pressure-based arrangement. Geometry-based redistribution of hydraulic energy is more effective and more sustainable than pressure-based intensification: when applied to a cleaning-limited bottomhole, intensification raises pump power without improving ROP and degrades E_s.

Future work will proceed in three phases: CFD-DEM simulation of the bit-bottomhole zone under non-Newtonian rheology benchmarked against this optimum (0-6 months); a laboratory flow-loop with an instrumented bit to calibrate k_c, β and ROP_{max} against data (6-12 months); and a field pilot with a drilling contractor comparing optimized and conventional arrangements (12-18 months). The model will also be extended to multi-nozzle arrangements with non-identical orientations.

Acknowledgements

The authors have not disclosed any funding.

Data availability

The datasets generated during and/or analyzed during the current study are available from the corresponding author on reasonable request.

Conflict of interest

The authors declare that they have no conflict of interest.

References

[1] D. K. Nazarbekova and B. N. Nurtoev, "Influence of the shape of drill bit nozzles in the flushing system of drilling tools to improve their bottomhole performance," (in Russian), *Oil and Gas Uzbekistan*, No. 2, pp. 32–41, 2025.

[2] D. K. Nazarbekova and B. N. Nurtoev, "Study of drilling fluids and their influence on nozzle orientation in the flushing system of drilling tools," (in Russian), *Inson Kapitali Va Mehnatni Muhofaza Qilish*, No. 2(5), pp. 305–310, 2025.

[3] D. Nazarbekova and B. Nurtoyev, "Comparative assessment of the effectiveness of methods to increase oil well productivity," in *AIP Conference Proceedings*, Vol. 3331, No. 1, p. 030029, Jan. 2025, https://doi.org/10.1063/5.0307221

[4] C.-C. Feng, Y. Li, W. Liu, and D.-L. Gao, "Optimization of rate of penetration through improved bit durability and extended directional nozzle," *Petroleum Science*, Vol. 22, No. 12, pp. 5114–5127, Dec. 2025, https://doi.org/10.1016/j.petsci.2025.10.007

[5] F. E. Dupriest and S. F. Noynaert, "Drilling practices and workflows for geothermal operations," in *IADC/SPE International Drilling Conference and Exhibition*, 2022, https://doi.org/10.2118/208798-ms

[6] Y. Liu, H. Zheng, and J. Zhang, "Optimization of nozzle spray angle and channel design to improve hydraulic energy distribution in roller cone bits," *Journal of Energy Resources Technology*, Vol. 145, No. 8, p. 082104, 2023.

[7] X. Meng, H. Zhou, H. Fan, Q. Peng, and S. Deng, "A systematic drilling hydraulics optimization method for improving rate of penetration and its application in ultra-deep wells," in *International Petroleum Technology Conference*, 2016, https://doi.org/10.2523/iptc-18829-ms

[8] M. Talipov, "Computational modeling and analysis of mechanical power consumption in train assemblers' work," in *Proceedings of the International Conference on Applied Innovation in IT*, Vol. 13, No. 2, pp. 419–426, 2025, https://doi.org/10.25673/120513

[9] M. Yakubov, M. Talipov, and U. Nurullaev, “An optimized Lagrangian approach to reactive power compensation in nonlinear traction power-supply systems,” *Vibroengineering Procedia*, Vol. 60, pp. 724–730, Dec. 2025, https://doi.org/10.21595/vp.2025.25604

[10] M. Schnuriger, B. Cuillier, D. Tilleman, and K. Rose, “Curved nozzle design for PDC bits enhances hydraulics for bit cleaning and cooling improvements,” in *SPE/IADC Drilling Conference and Exhibition*, 2017, https://doi.org/10.2118/184734-ms

[11] S. Akhshik, M. Behzad, and M. Rajabi, “CFD-DEM simulation of the hole cleaning process in a deviated well drilling: The effects of particle shape,” *Particuology*, Vol. 25, No. 1, pp. 72–82, 2016, https://doi.org/10.1016/j.partic.2015.02.008

[12] C. Cai et al., “Non-spherical debris cuttings-carrying performance in PDC bits with CFD-DEM coupling method,” *Chemical Engineering Research and Design*, Vol. 230, pp. 390–403, 2026, https://doi.org/10.1016/j.cherd.2026.04.048

[13] Z. Chen et al., “Hydraulic parameters optimization of two-stage PDC bit in deep formation applications,” *Geoenergy Science and Engineering*, Vol. 230, p. 212248, Nov. 2023, https://doi.org/10.1016/j.geoen.2023.212248

[14] W. Hu, N. Guan, J. Zhang, B. Xu, and H. Zhu, “A novel critical velocity model for the incipient motion of non-spherical particles on cuttings bed in extended reach wells,” *Particuology*, Vol. 97, No. 3, pp. 193–206, 2025, https://doi.org/10.1016/j.partic.2024.12.011

[15] A. Seryakov, Y. Ignatenko, and O. B. Bocharov, “Characteristics of a particle’s incipient motion from a rough wall in shear flow of Herschel-Bulkley fluid,” *Fluids*, Vol. 9, No. 3, p. 65, 2024, https://doi.org/10.3390/fluids9030065

[16] L. Esfahanizadeh, B. Dabir, and F. Goharpey, “CFD modeling of the flow behavior around a PDC drill bit: effects of nano-enhanced drilling fluids on cutting transport and cooling efficiency,” *Engineering Applications of Computational Fluid Mechanics*, Vol. 16, No. 1, pp. 977–994, Dec. 2022, https://doi.org/10.1080/19942060.2022.2026821